# Supporting Information

# From Plastic Waste to Value-Added Chemicals: A Trimetallic MOF Strategy for Electrochemical PET Upcycling

Divy G. Solanki[1], Pooja J. Sharma[1], Sanjay A. Bhakhar[1], Manish N. Nandpal[2], Samir G. Patel[2], Chakkooth Vijayakumar[3], Sudhanshu Sharma[4], C.K. Sumesh[1], Pratik M. Pataniya[1*]

[1]*Department of Physical Sciences, P. D. Patel Institute of Applied Sciences, Charotar University of Science & Technology, CHARUSAT, Changa, India-388421.*

[2]*Department of Pharmaceutical Chemistry and Analysis, Ramanbhai Patel College of Pharmacy, Charotar University of Science and Technology, CHARUSAT Changa-388421, India.*

[3]*Chemical Sciences and Technology Division, CSIR-National Institute for Interdisciplinary Science and Technology (NIIST), Thiruvananthapuram-695 019, India.*

[4]*Department of Chemistry, Indian Institute of Technology Gandhinagar, Palaj, 382355, India.*

[*]**Email:** pm.pataniya9991@gmail.com

**Synthesis of PET hydrolysate:**

Firstly, the waste PET bottle was cut into small pieces of dimensions 5-7 mm. The 4g of PET waste were added into 50 ml of 2M KOH aqueous solution. This mixture was then transferred into SS-lined Teflon autoclave (capacity: 100 ml) and heated at 160 °C for 15 hours. The clear hydrolysate was finally collected and diluted to 1M KOH by adding 50 ml distilled water into prepared hydrolysate.

**Materials characterizations:**

The structural properties of the as synthesized Co-MOF, NiMn@Co-MOF and NiMn@NF electrodes were characterized by powder X-ray diffraction (XRD) using a Bruker D2 Phaser diffractometer with Cu Kα radiation (λ = 1.54184 Å). The surface morphology and elemental composition were examined using field-emission scanning electron microscopy (FE-SEM, Phenom Pharos G2) coupled with an energy-dispersive X-ray spectrometer (EDS). Raman spectra were recorded with an i-Raman Plus spectrometer (Metrohm Group). The surface chemical composition was further studied using X-ray photoelectron spectroscopy (XPS).

**Electrochemical measurements:**

A standard three-electrode set-up with as-prepared Co-MOF, NiMn@Co-MOF and NiMn@NF electrodes as working electrodes, Ag/AgCl electrode (saturated with 3 M KCl) as the reference, and a platinum wire as the counter electrode was used to analyse the electrochemical properties. The Metrohm PGSTAT-M204 electrochemical workstation was used for electrochemical measurements in 1M KOH electrolyte with and without EG, and PET hydrolysate. All the potentials were calculated with respect to the reversible hydrogen electrode (RHE):

$E(RHE) = E_{Ag/AgCl} + 0.1976 + (0.059 \times pH)$

The linear sweep voltammetry (LSV) curves were recorded at scan rate of 5mV/s. The polarization curves were measured with 90% of iR-compensation. The Tafel slope was calculated to study the reaction kinetics and to determine the rate determining step (RDS). The charge-transport behaviour of electrodes was analysed using electrochemical impedance spectroscopy (EIS). The cyclic-voltammetry curves were recorded in non-faradaic region at different scan rate 10-100 mV/s. The double layer capacitance ($C_{dl}$) was determined to study the electrochemically active surface area (ECSA). To study the surface reconstruction and mechanism of OER and EGOR, in-situ operando EC-Raman spectroscopy was accomplished using i-Raman Plus spectrometer (Metrohm Group) and VIONIC EC-workstation (Metrohm) having 532 nm photo-excitation. The chrono-amperometry and chrono-potentiometry tests were accomplished to study the stability of the long-term electrolysis for PET-upcycling.

The specific capacitance (Cs) was calculated using following equation[1]:

$$C_s = \frac{\int_{V1}^{V2} I dV}{2\eta \Delta V} \quad (1)$$

Here $\int_{V1}^{V2} I\, dV$ is the area of CV loops, η is the scan rate (V/s), and $\Delta V$ is potential window.

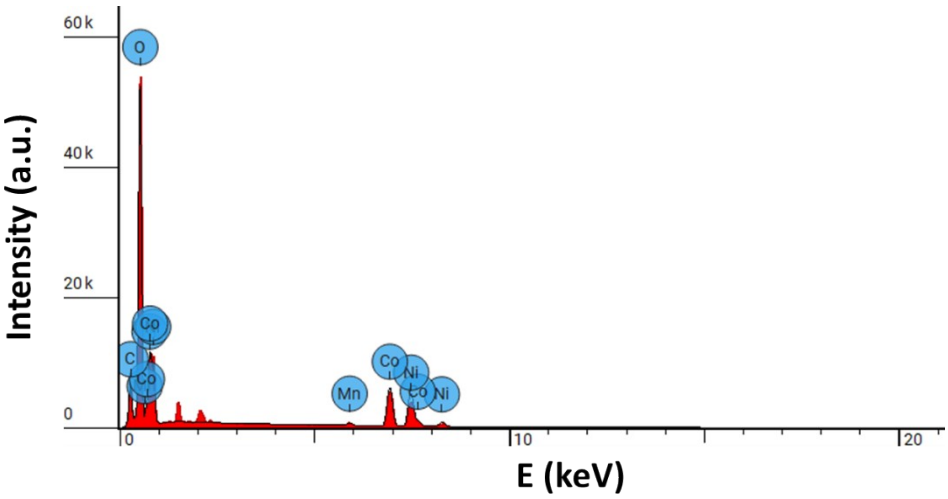


**Figure S1** EDS pattern of NiMnCo-MOF.

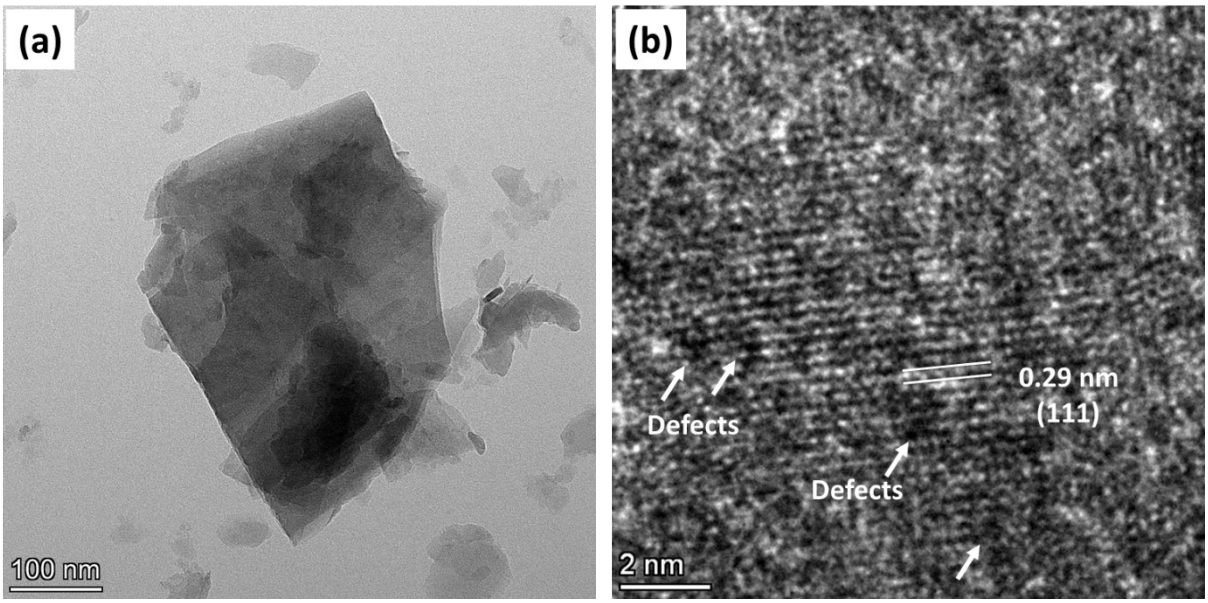


**Figure S2** (a) TEM image, (b) HR-TEM image of NiMnCo-1.

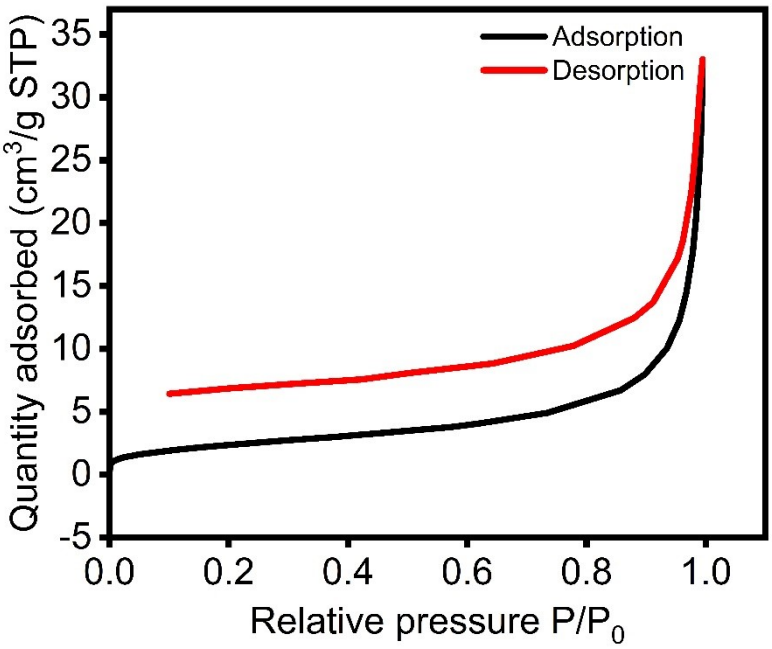


**Figure S3** Brunauer-Emmett-Teller (BET) analysis: a nitrogen adsorption-desorption isotherms and pore size distribution of NiMnCo-1 electrocatalyst.

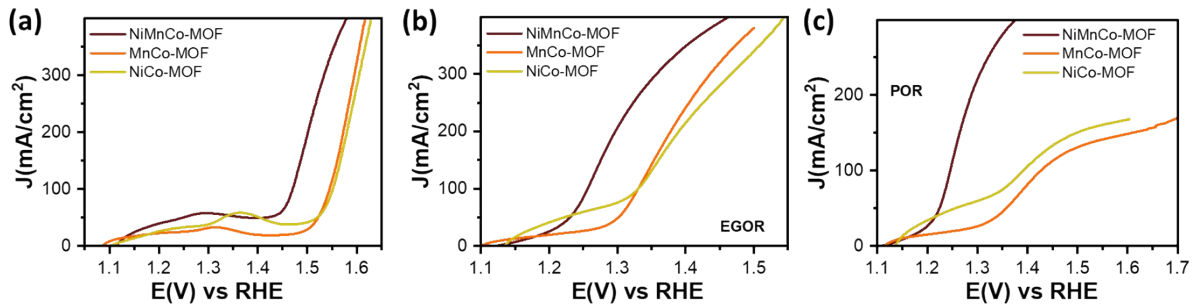


**Figure S4** Polarization curves for NiMnCo-1, MnCo-MOF and NiCo-MOF for (a) OER, (b) EGOR (1M KOH + 0.3M EG), and (c) POR (PET hydrolysate).

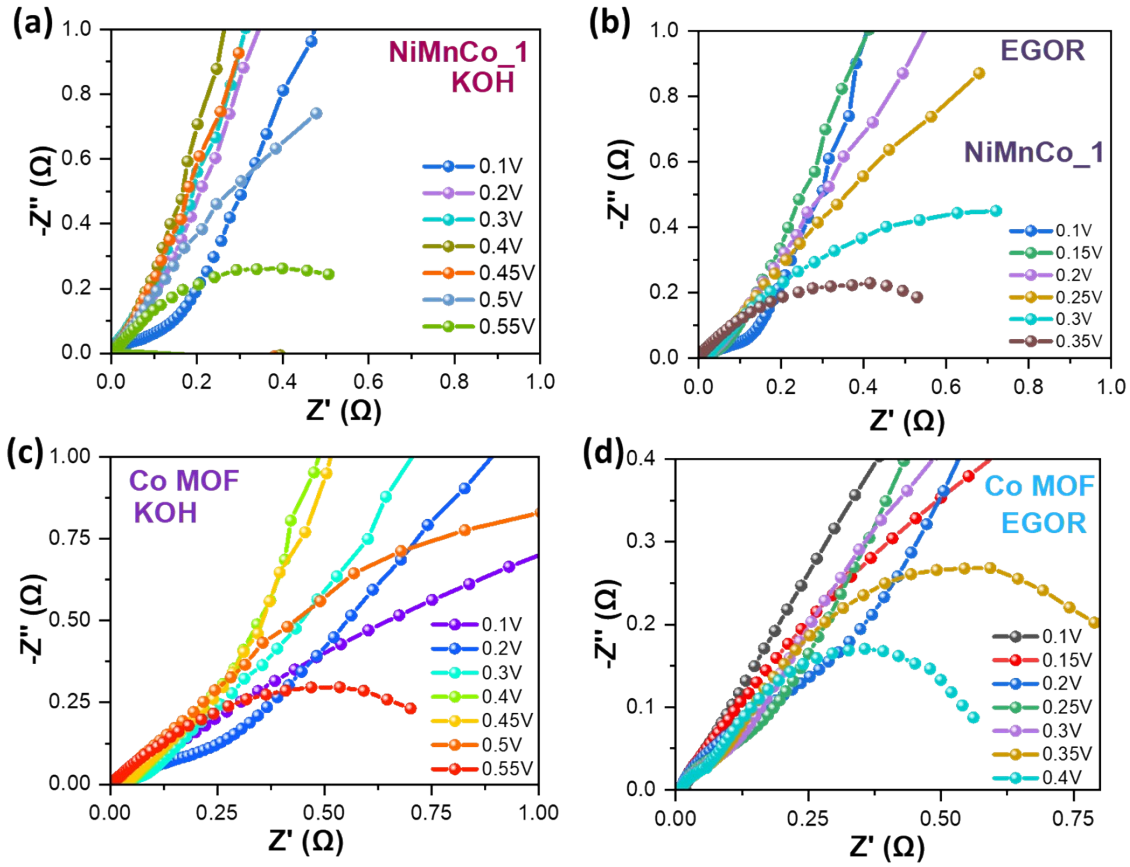


**Figure S5** Nyquist plots for Co-MOF and NiMnCo-MOF for OER and EGOR.

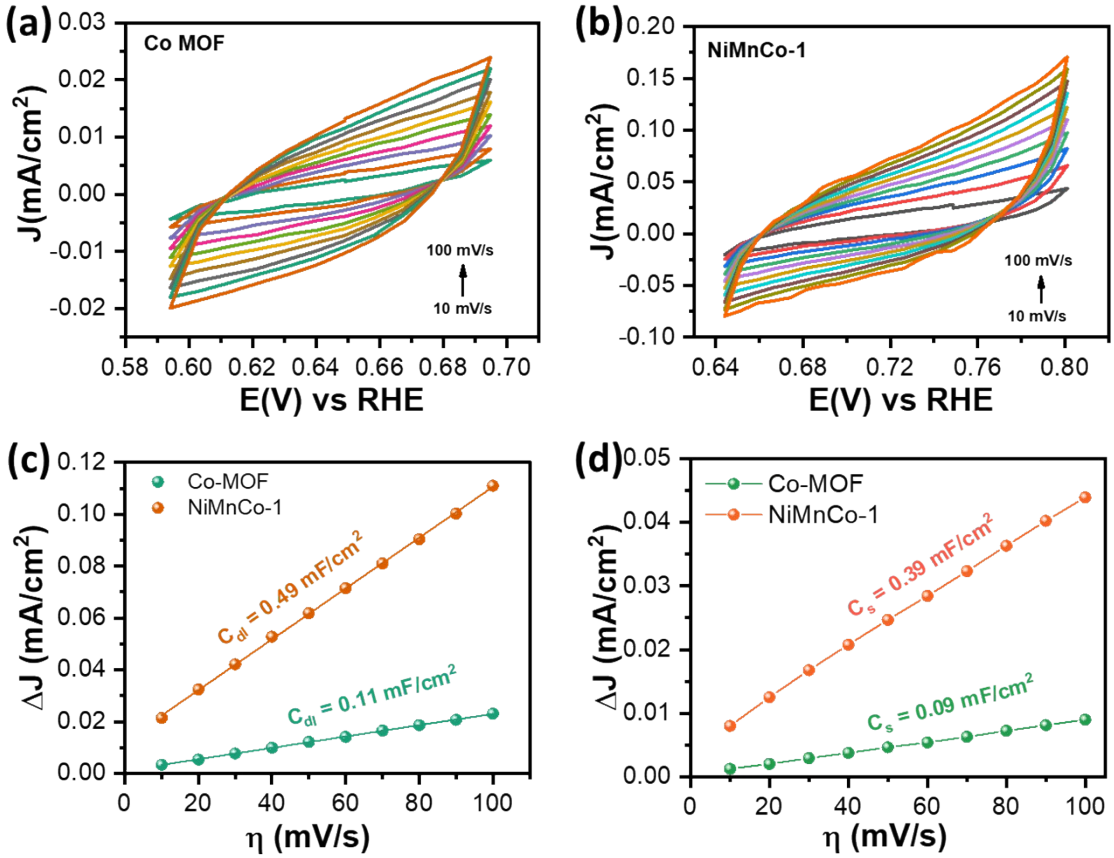


**Figure S6** CV curves in non-faradic potential range (a) for Co MOF and (b) NiMnCo-1, (c) ΔJ vs scan rate (η) for evaluation of double layer capacitance ($C_{dl}$), (d) ΔJ vs scan rate (η) for evaluation of specific capacitance ($C_s$)for Co MOF and NiMnCo-1.

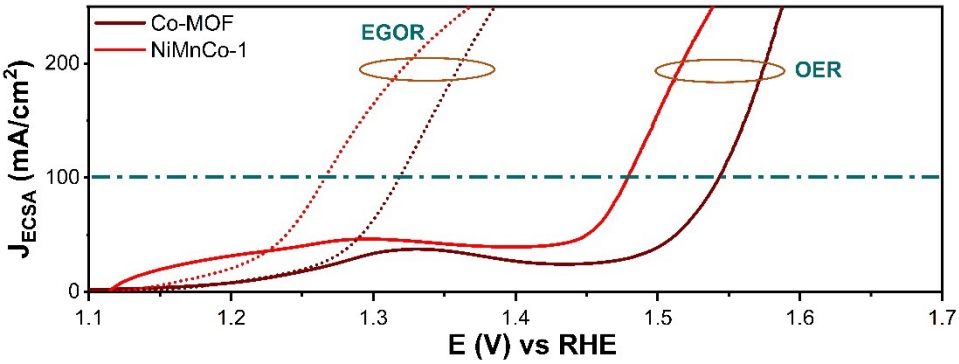


**Figure S7** Normalized polarization curves OER and EGOR performance of Co-MOF and NiMnCo-1.

**Table S1** Optimized Chromatographic Conditions.

| Parameters | Experimental conditions |
|---|---|
| Instrument | Shimadzu High-Performance Liquid Chromatographic System, Japan (LC-2010 CHT), equipped with PDA detector fitted with quaternary gradient pump, degasser, column oven and autosampler |
| Column | Luna $C_{18}$ Column (250 mm×4.6 mm; 5µm) |
| Mobile phase | 27.5 mM $H_2SO_4$<br>(0.75 mL of $H_2SO_4$ in 500 mL of Milli-Q Water) |
| Mobile phase Ratio | 100 % v/v |
| Flow rate | 0.3 mL/min |
| Diluent | Milli-Q Water |
| Injection volume | 20 µL |
| Column oven temperature | 35 ºC |
| Auto sampler temperature | 15 ºC |
| Detector | Photo Diode Array (PDA) |
| Lamp | $D_2$ |
| Detection wavelength | 210 nm |
| Software | LabSolutions |
| Run time | 20 minutes |
| These were optimized chromatographic conditions which gives satisfactory results and lie well within acceptance criteria. | |

.

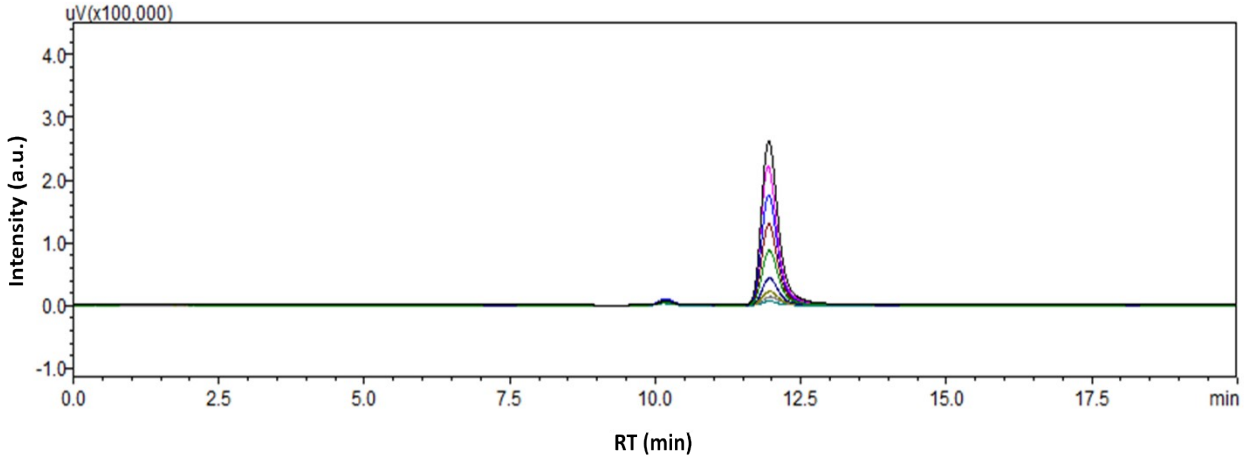


**Figure S8** Chromatographs of standard formate solution for calibration.

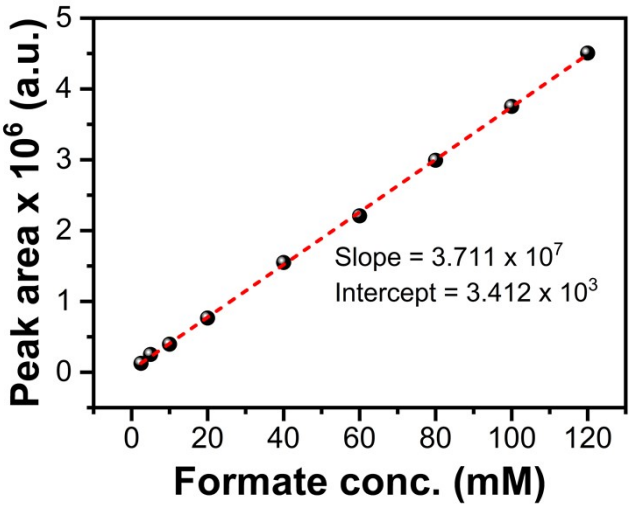


**Figure S9** Calibration curve for quantification of formate.

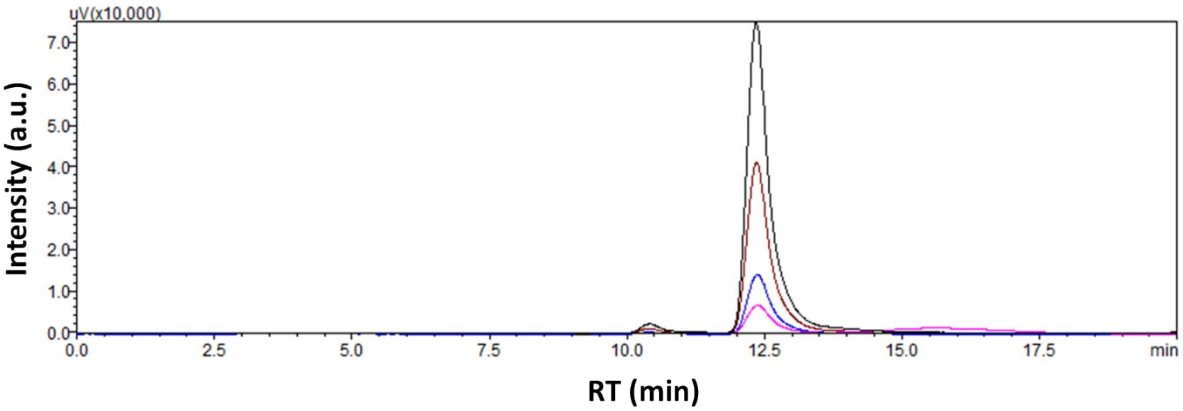


**Figure S10** Chromatographs of EG electrolyte after electrolysis at different current densities (10, 20, 50 and 100 mA/cm$^2$) for 2 hours.

The Faradaic efficiency (FE) for the EG to formate conversion can be calculate using **equation: S1**,

$$FE\ (\%) = \frac{3\ \times\ HCOO^-\,(mol) \times 96485\ (C/mol)}{Total\ charge} \times 100\%$$

(S1)

**Table S2** Quantification of formate and Faradaic efficiency.

| Current density (mA/cm$^2$) | Charge (C) | Formate production rate (m mol cm$^{-2}$ h$^{-1}$) | FE (%) |
|---|---|---|---|
| 10 | 72 | 0.092 | 74 |
| 20 | 144 | 0.219 | 88 |
| 50 | 360 | 0.590 | 95 |

| | | | |
|---|---|---|---|
| 100 | 720 | 1.218 | 98 |

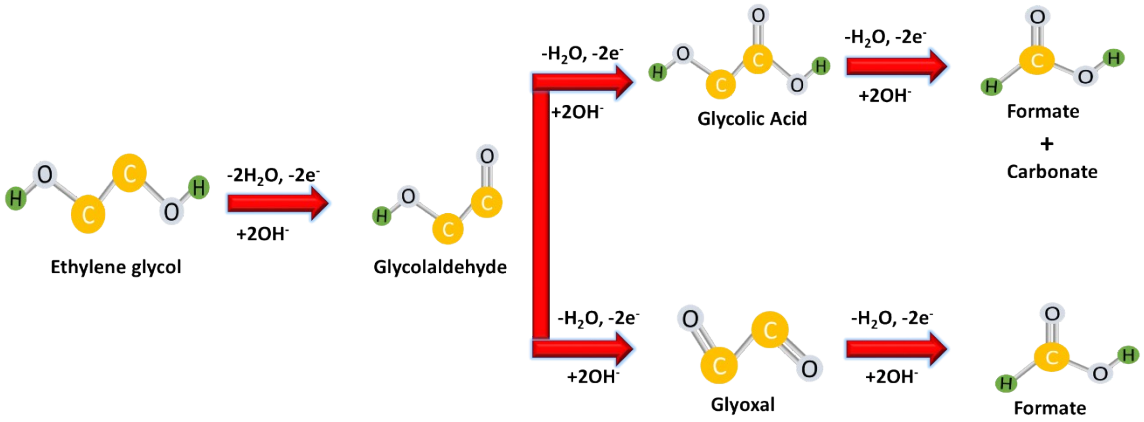


**Figure S11** Schematic diagram of EG oxidation pathways in alkaline electrolyte.

**Table S3** Comparison of PET electrolysis performance of NiMnCo-MOF with previous reports.

| Catalysts | PET treatment and Measurement condition | Potential (V)@current density | Anode FE (%) (Formate) | Ref. |
|---|---|---|---|---|
| NiMnCo-MOF | 4 g PET Bottle + 50 ml 2M KOH 150°C for 15 hr [single cell] | 1.25V vs RHE@ 100 mA/cm$^2$ | 98% @ 100 mA/cm$^2$ | **This work** |
| Ce-NiCoS | 4 g PET Bottle + 50 ml 2M KOH 150°C for 15 hr [single cell] | 1.39 V @ 10 mA/cm$^2$ 1.61 V @ 100 mA/cm$^2$ | 97% @10 mA/cm$^2$ | [2] |
| Ni-$Fe_3Se_4$ | 4 g PET Bottle + 50 ml 2M KOH 150°C for 15 hr [single cell] | 1.49 V @ 10 mA/cm$^2$ 1.60 V @ 50 mA/cm$^2$ | 89% @50 mA/cm$^2$ | [3] |
| NiCe@NiTe | 4 g PET Bottle + 50 ml 2M KOH 150°C for 15 hr [single cell] | 1.55 V @ 10 mA/cm$^2$ | 96.5%@10 mA/cm$^2$ 85.8%@ 20 mA/cm$^2$ | [4] |
| OMS-$Ni_1$-CoP | 6.3 g PET + 100 ml 2M KOH [Single cell] | 1.52 V @ 10 mA/cm$^2$ | 96% | [5] |
| $CuCo_2O_4$/NF | 5g PET + 50 ml 5M KOH [Membrane electrode assembly (MEA) flow cell] | 1.56 V @ 100 mA/cm$^2$ | 93% | [6] |
| $Ni_3N/W_5N_4$ | 2.0 g PET bottle + 100 | 1.47 V @ 50 | 85% | [7] |

| | | | | |
|---|---|---|---|---|
| | ml 4M KOH [AEM H-type cell] | mA/cm$^2$ | | |
| $NiCo_2O_4$/CFP | 0.768 g PET powder was added in 40 mL of 1 M NaOH solution and autoclaved at 180°C for 2 h. [ H-type cell (anion exchange membrane, AEM)] | 1.9 V @ 20 mA/cm$^2$<br><br>Cathode:$CO_2$RR | 90% | [8] |
| CuO nanowire | 0.77 g PET powder was added in 40 mL of 1 M KOH solution and autoclaved at 180°C for 2h | -<br>[H-type cell] | 88% | [9] |

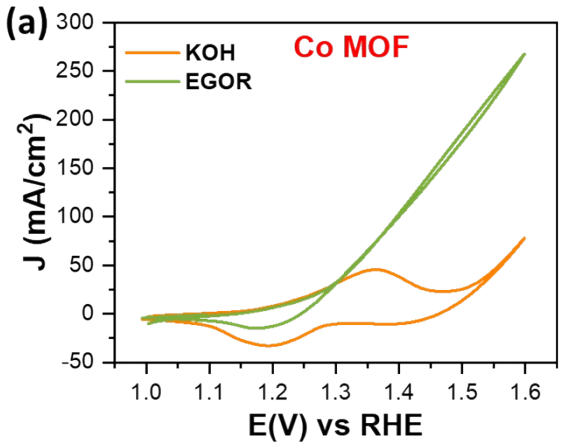


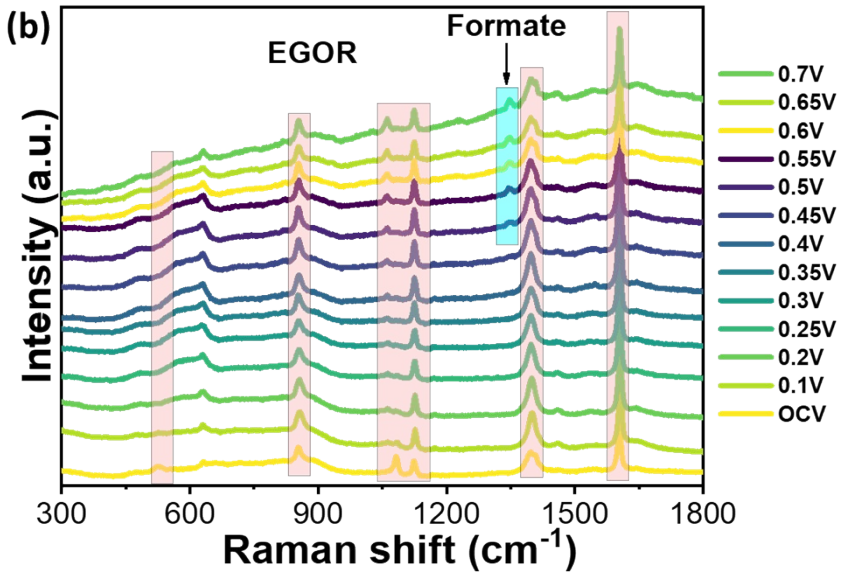

**Figure S12** (a) CV curves of Co-MOF in 1 M KOH with and without 0.3 M EG and (b) In-situ Raman spectra of Co-MOF in 1 M KOH with 0.3 M EG.

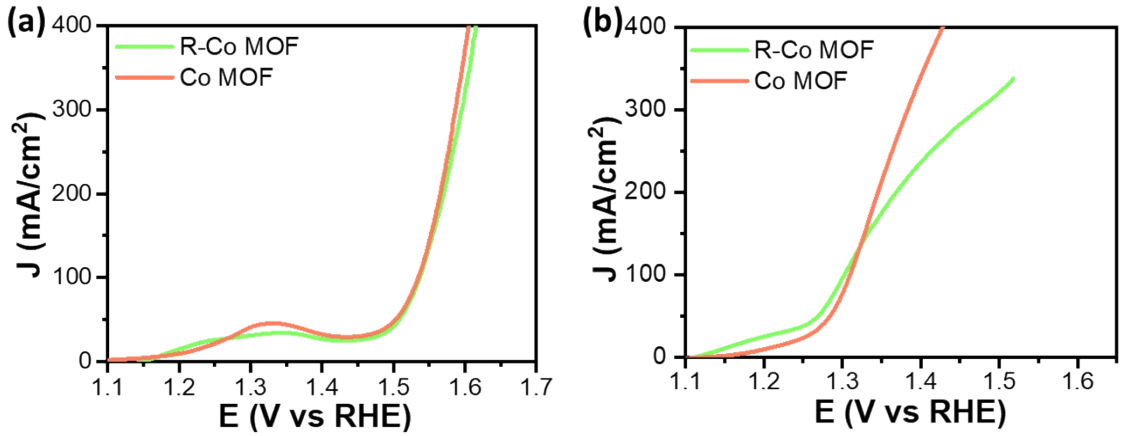


**Figure S13** Polarization curves for R-Co-MOF (prepared with recovered TPA) and Co-MOF (a) for OER and (b) for EGOR performance.

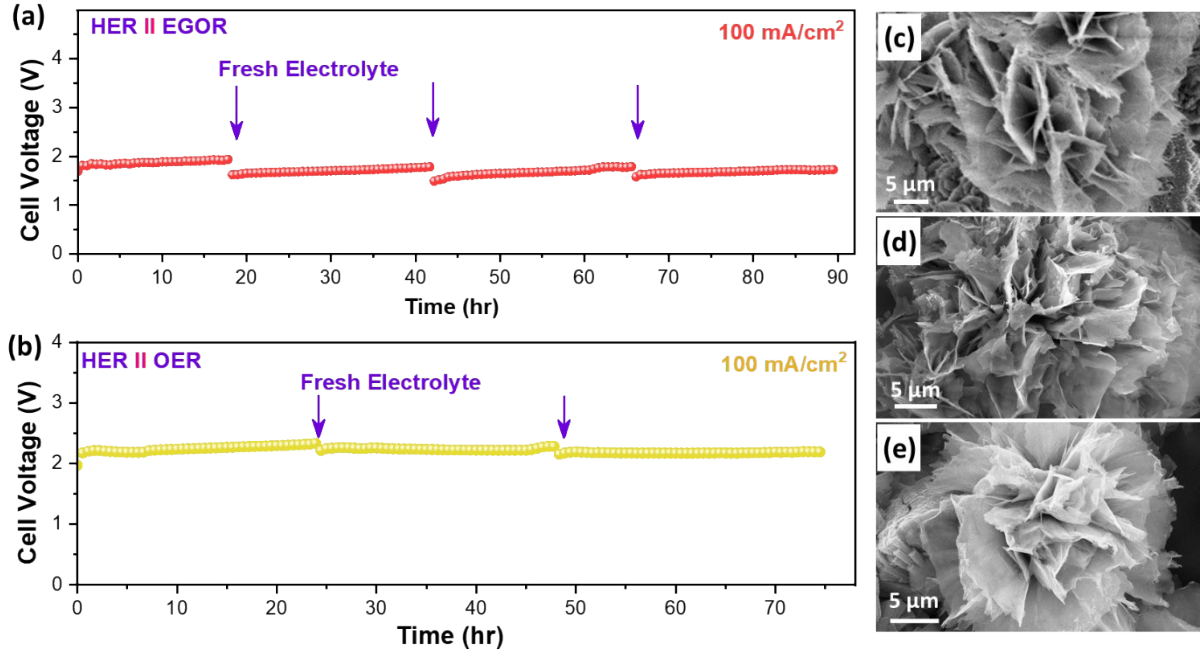


**Figure S14** Chrono-potentiometry curve at 100 mA/cm$^2$ for study of stability of NiMnCo-MOF (a) in 1M KOH+0.3 M EG, (b) in 1M KOH and SEM images of NiMnCo-MOF (c) before electrolysis, (d) after OER, (e) after EGOR.

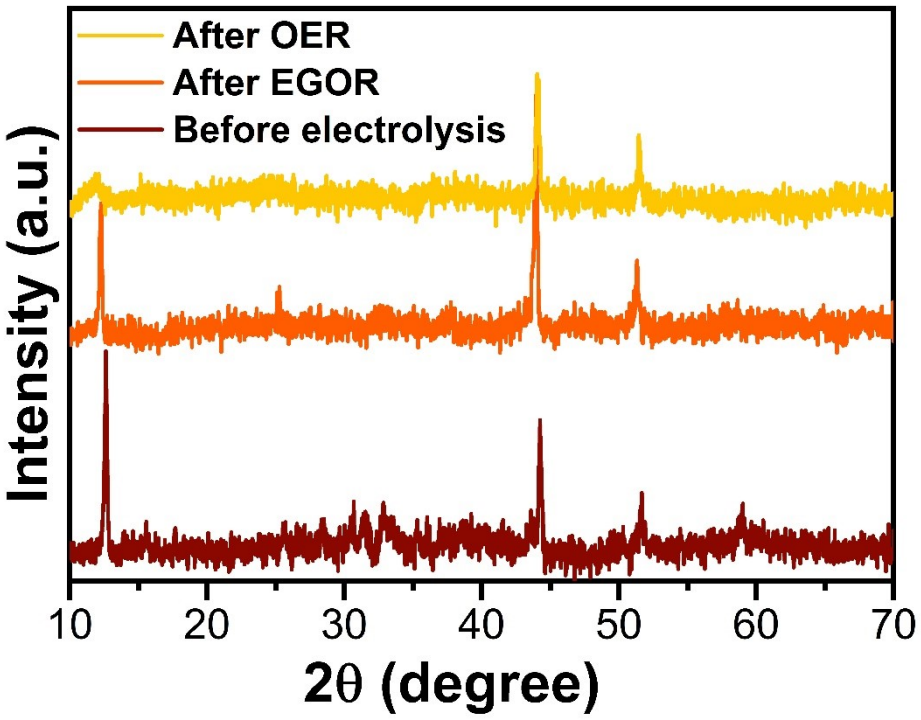


**Figure S15** Powder XRD patterns of NiMnCo-1 before electrolysis, after OER and after EGOR performance.

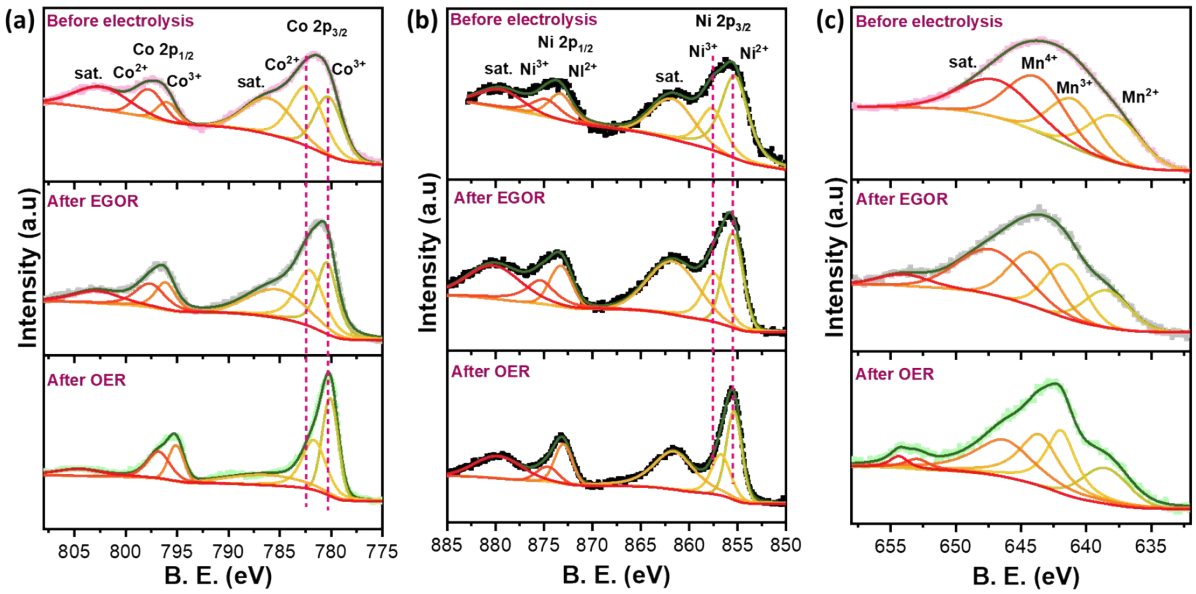


**Figure S16** Post-stability XPS survey after EGOR and OER performance (a) Co 2p, (b) Ni 2p, and (c) Mn 2p for NiMnCo-1 electrocatalyst.

**References:**


[1] D. Xiong, X. He, Z. Zhu, T. Liu, D. Wu, Y. Zou, Z. Chen, Upcycling Polybutylene Succinate Waste to Succinic Acid via Paired Electrocatalytic using Thiol-Engineered MOFs and a CO2-Assisted Precipitation System, Adv. Funct. Mater. 36 (2026) e18434. https://doi.org/https://doi.org/10.1002/adfm.202518434.

[2] P.M. Pataniya, P.J. Sharma, S.A. Bhakhar, N. Rajani, M.N. Nandpal, K.A. Bhakhar, S.G. Patel, C. Vijayakumar, S. CK, Coupling Polyethylene Terephthalate Plastic Upcycling and Hydrogen Evolution Using Cerium-Doped Nickel Cobalt Sulfide Electrocatalysts, ACS Appl. Mater. Interfaces. 18 (2026) 1843–1853. https://doi.org/10.1021/acsami.5c22894.

[3] P.J. Sharma, S.A. Bhakhar, M.N. Patel, M.N. Nandpal, K.A. Bhakhar, S.G. Patel, P. Sahatiya, G. Nagaraju, C.K. Sumesh, P.M. Pataniya, Binder-free nickel–iron selenide catalyst arrays for coupling hydrogen production with polyethylene terephthalate plastic electro-upcycling, J. Mater. Chem. A. 14 (2026) 1923–1935. https://doi.org/10.1039/D5TA06515A.

[4] P.J. Sharma, S.A. Bhakhar, M.N. Nandpal, K.A. Bhakhar, S.G. Patel, P. Sahatiya, C.K. Sumesh, P.M. Pataniya, Electro-upcycling of PET plastic coupled with hydrogen production using the NiCe@NiTe electrocatalyst, J. Mater. Chem. A. 14 (2026) 3591–3604. https://doi.org/10.1039/D5TA08195E.

[5] N. Wang, X. Li, M.-K. Hu, W. Wei, S.-H. Zhou, X.-T. Wu, Q.-L. Zhu, Ordered macroporous superstructure of bifunctional cobalt phosphide with heteroatomic modification for paired hydrogen production and polyethylene terephthalate plastic recycling, Appl. Catal. B Environ. 316 (2022) 121667. https://doi.org/https://doi.org/10.1016/j.apcatb.2022.121667.

[6] F. Liu, X. Gao, R. Shi, E.C.M. Tse, Y. Chen, A general electrochemical strategy for upcycling polyester plastics into added-value chemicals by a CuCo2O4 catalyst, Green Chem. 24 (2022) 6571–6577. https://doi.org/10.1039/D2GC02049A.

[7] F. Ma, S. Wang, X. Gong, X. Liu, Z. Wang, P. Wang, Y. Liu, H. Cheng, Y. Dai, Z. Zheng, B. Huang, Highly efficient electrocatalytic hydrogen evolution coupled with upcycling of microplastics in seawater enabled via Ni3N/W5N4 janus nanostructures, Appl. Catal. B Environ. Energy. 307 (2022) 121198. https://doi.org/https://doi.org/10.1016/j.apcatb.2022.121198.

[8] J. Wang, X. Li, M. Wang, T. Zhang, X. Chai, J. Lu, T. Wang, Y. Zhao, D. Ma, Electrocatalytic Valorization of Poly(ethylene terephthalate) Plastic and CO2 for Simultaneous Production of Formic Acid, ACS Catal. 12 (2022) 6722–6728. https://doi.org/10.1021/acscatal.2c01128.

[9] J. Wang, X. Li, T. Zhang, Y. Chen, T. Wang, Y. Zhao, Electro-reforming polyethylene terephthalate plastic to co-produce valued chemicals and green hydrogen, J. Phys. Chem. Lett. 13 (2022) 622–627.